

Supporting information

Enhancing the Stability and Efficiency of Carbon-Based Perovskite Solar Cell Performance with ZrO₂-Decorated rGO Nano-sheets in a Mesoporous TiO₂ Electron Transport Layer

Anjan Kumar¹, M. I. Sayyed^{2,3}, Anmar Ghanim Taki^{4*}, Vanessa Valverde⁵, Eduardo Hernández⁶

¹Department of Electronics and Communication, GLA University, Mathura-281406, India

²Department of Physics, Faculty of Science, Isra University, Amman 11622, Jordan

³ Renewable Energy and Environmental Technology Center, University of Tabuk, Tabuk 47913, Saudi Arabia.

⁴ Department of Radiology & Sonar Techniques, Al-Noor University College, Nineveh, Iraq

⁵Facultad Mecánica, Escuela Superior Politécnica de Chimborazo (ESPOCH), Riobamba, 060155, Ecuador

⁶Facultad Mecánica, Escuela Superior Politécnica de Chimborazo (ESPOCH), Riobamba, 060155, Ecuador.

*Corresponding author email: anmar.ghanim@alnoor.edu.iq

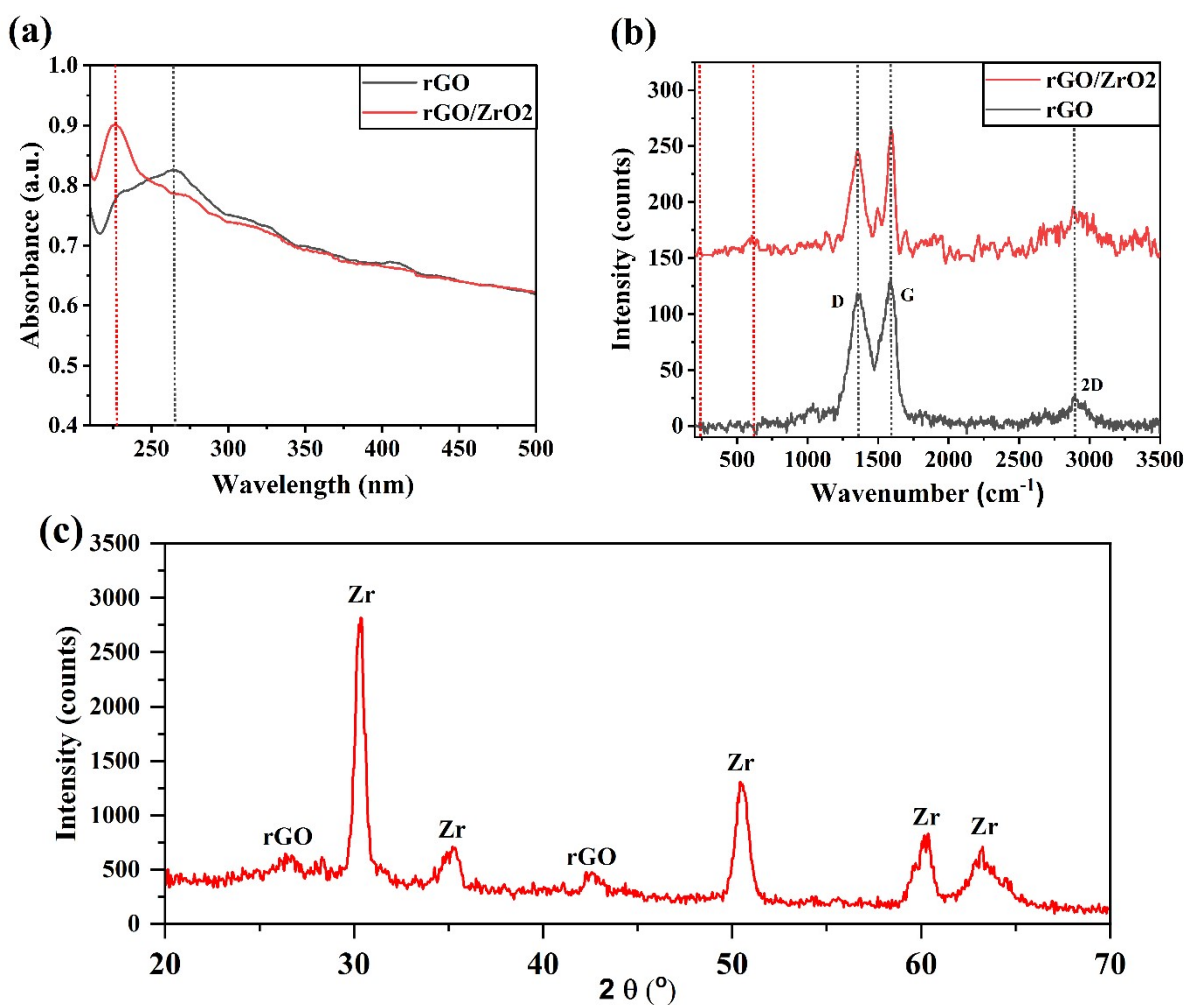


Figure S1. (a) UV-Vis and (b) RAMAN spectra of rGO and rGO/ZrO₂ materials. (c) XRD pattern of rGO/ZrO₂ nanocomposite.

Note 1:

Figure S1a shows the absorbance spectra of rGO and rGO/ZrO₂ materials. While rGO material has a peak at 265 nm, the rGO/ZrO₂ nanocomposite has two peaks at 227 nm related to the ZrO₂ phase and a shoulder peak at 273 nm related to the rGO phase. Figure S1b shows the RAMAN spectra of samples. As shown, in rGO/ZrO₂ profile, in addition to rGO RAMAN peaks an additional peak at 603 cm⁻¹ related to ZrO₂ NPs is observed. Notably, the I_D/I_G ratio for rGO is 0.90, higher than the 0.81 calculated for rGO/ZrO₂ material. It indicates that during the synthesis process of rGO/ZrO₂, regions of sp² would be enlarged, which increases the electrical conductivity of rGO derivatives. This phenomenon agrees with the redshift of absorbance peak of rGO in rGO/ZrO₂. Successful synthesis of rGO/ZrO₂ nanocomposite is approved with presence of ZrO₂ phase in XRD pattern of rGO/ZrO₂ (Figure S1c).

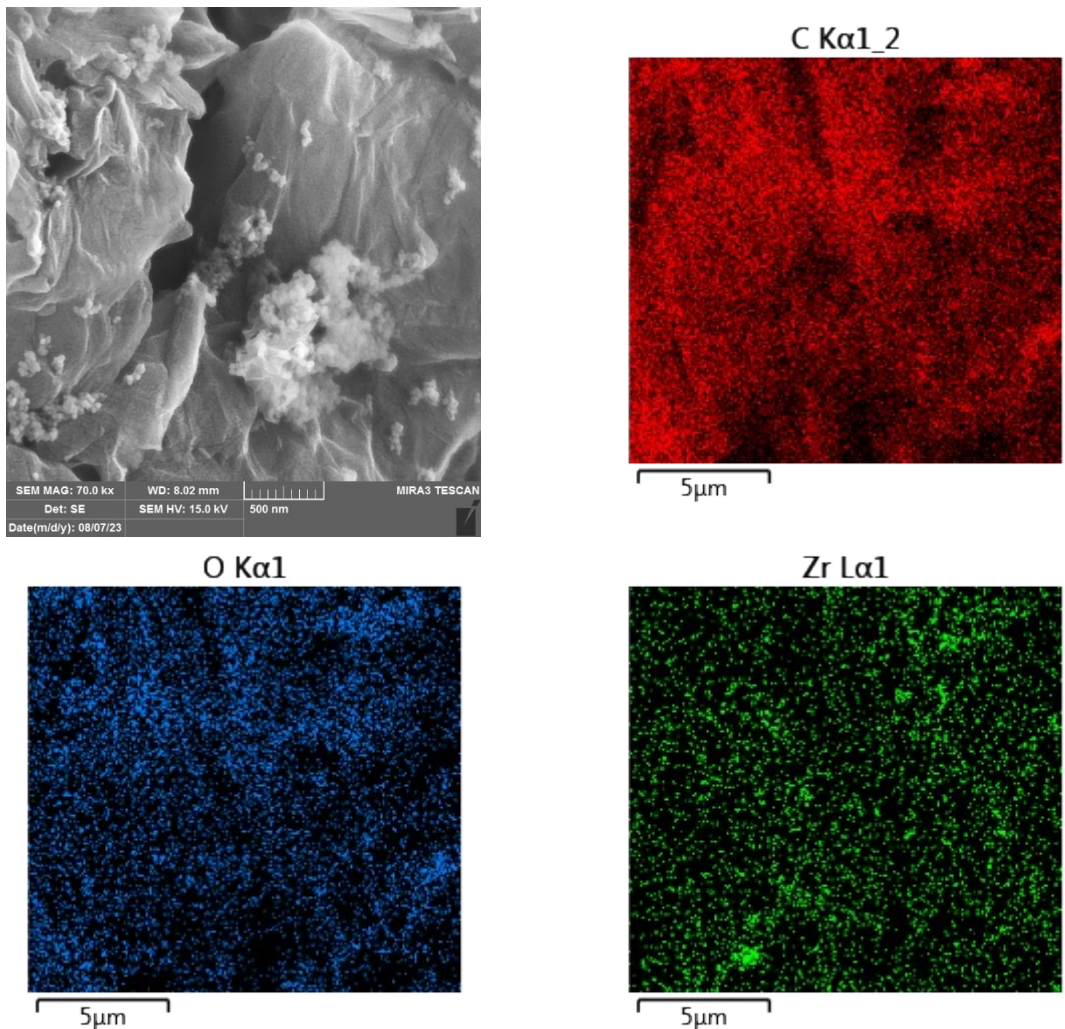


Figure S2. FESEM image of rGO/ZrO₂ nanocomposite with related elemental mapping.

Note 2:

Figure S2 shows the FESEM image of rGO/ZrO₂ nanocomposite. As can be seen, nanocomposites have wrinkle sheets that are covered with ZrO₂ NPs. In addition, the elemental mapping analysis of rGO/ZrO₂ for C, O, and Zr reveals that the ZrO₂ NPs nanoparticles were homogeneously distributed on the rGO sheets. Elemental mapping results approve the successful formation of rGO/ZrO₂ nanocomposites.

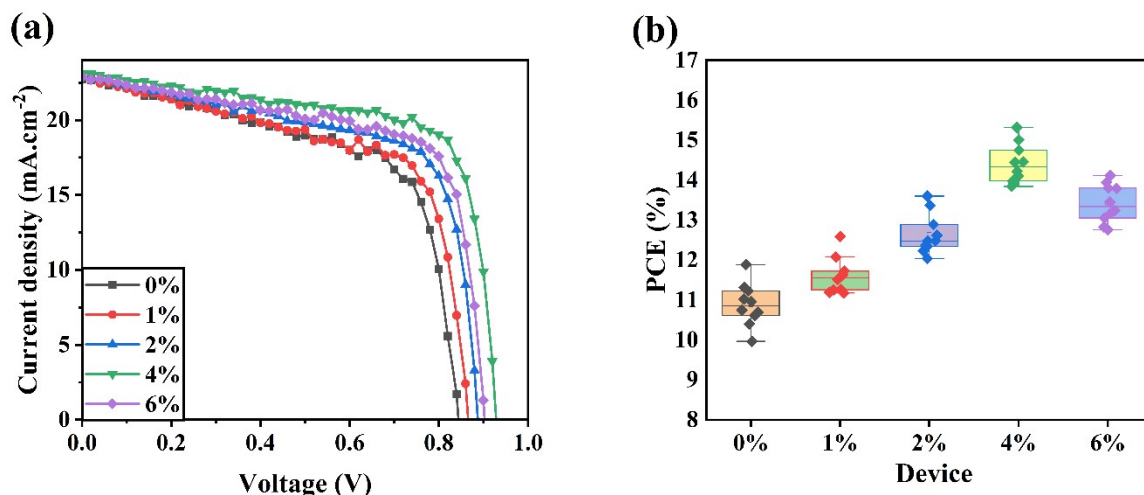


Figure S3. (a) J-V curves and (b) PCE distributions of fabricated HTL-free CPSCs with ETLs doped with different amounts of rGO/ZrO₂ dopant.

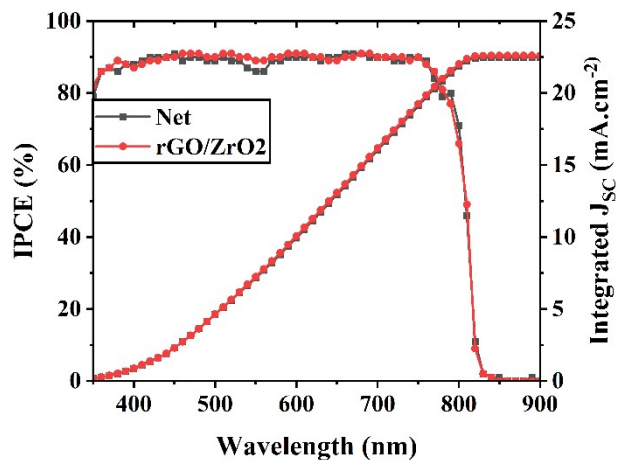


Figure S4: IPCE spectra of net and rGO/ZrO₂ HTL-free CPSCs with related integrated current density.

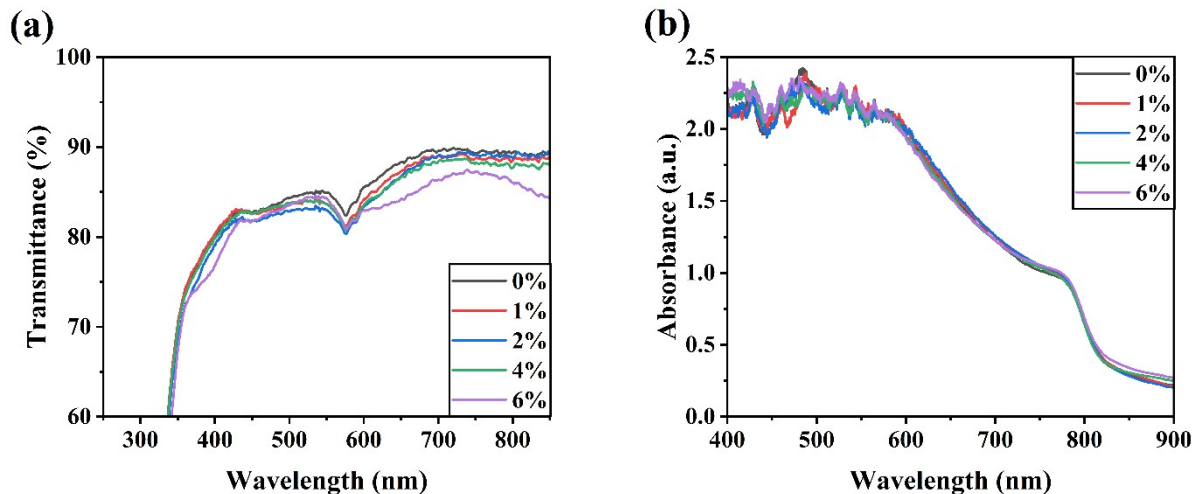


Figure S5. (a) Transmittance of ETLs doped with different amounts of rGO/ZrO₂ nanocomposite. (b) Absorbance of perovskite layers fabricated ETLs doped with different amounts of rGO/ZrO₂ dopant.

Table S1. Photovoltaic parameters of fabricated HTL-free CPSCs with ETLs doped with different amounts of rGO/ZrO₂ dopant.

Device name		V _{OC} (V)	J _{SC} (mA.cm ⁻²)	FF (%)	PCE (%)
0%	Average	0.816	22.61	58.96	10.88
	Best	0.850	22.79	61.32	11.88
1%	Average	0.836	22.57	61.47	11.60
	Best	0.870	22.88	63.27	12.59
2%	Average	0.866	22.60	64.54	12.64
	Best	0.890	22.86	66.84	13.60
4%	Average	0.900	22.74	70.31	14.39
	Best	0.930	23.11	70.76	15.21
6%	Average	0.884	22.65	66.98	13.41
	Best	0.910	22.89	67.76	14.12

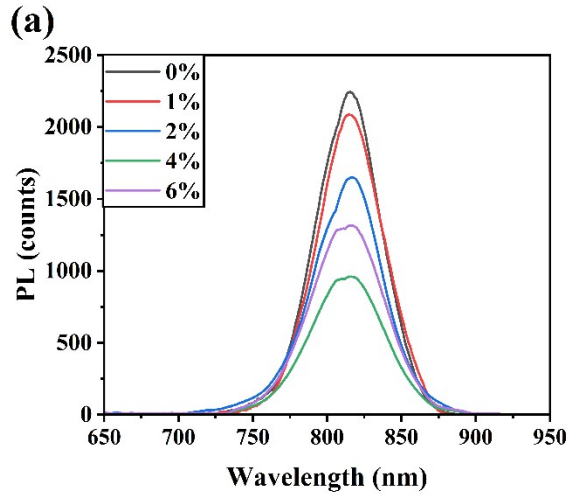


Figure S6. PL spectra of fabricated perovskite layers on ETLs doped with different amounts of rGO/ZrO₂ dopant.

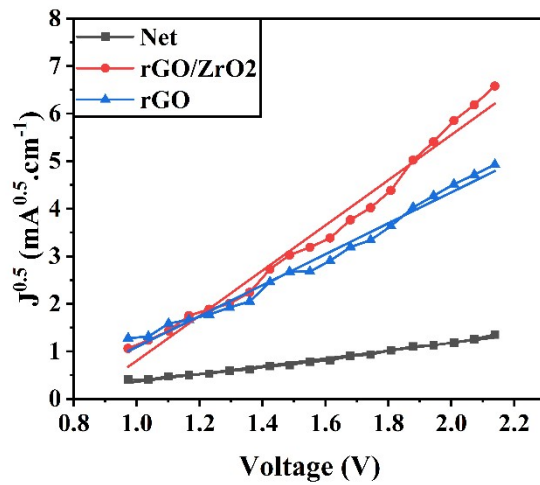


Figure S7. J^{0.5}-V of different hole only devices with different ETLs

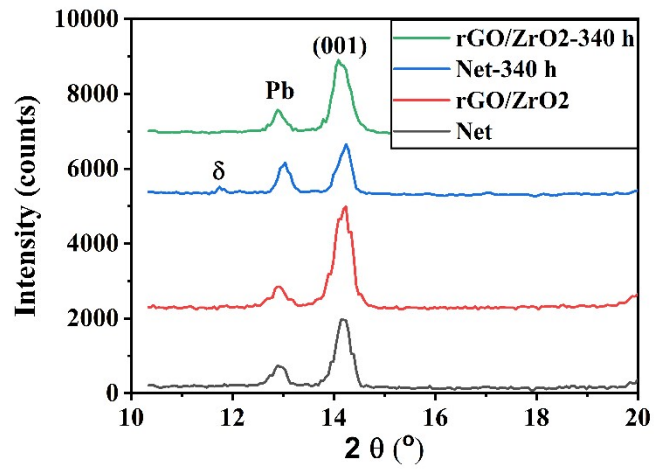


Figure S8. XRD pattern of perovskite layers during aging at a temperature of 50 °C in ambient air with a relative humidity of 25-30% for 340 h.